Biophysical Journal Volume 107 October 2014 1712–1720

Article

Bacterial Motility Patterns Reveal Importance of Exploitation over Exploration in Marine Microhabitats. Part I: Theory

Li Xie[1] and Xiao-Lun Wu[1,*]
[1]Department of Physics and Astronomy, University of Pittsburgh, Pittsburgh, Pennsylvania

ABSTRACT Bacteria use different motility patterns to navigate and explore natural habitats. However, how these motility patterns are selected, and what their benefits may be, are not understood. In this article, we analyze the effect of motility patterns on a cell's ability to migrate in a chemical gradient and to localize at the top of the gradient, the two most important characteristics of bacterial chemotaxis. We will focus on two motility patterns, run-tumble and run-reverse-flick, that are observed and characterized in enteric bacterium *Escherichia coli* and marine bacterium *Vibrio alginolyticus*, respectively. To make an objective comparison, master equations are developed on the basis of microscopic motions of the bacteria. An unexpected yet significant result is that by adopting the run-reverse-flick motility pattern, a bacterium can reduce its diffusivity without compromising its drift in the chemical gradient. This finding is biologically important as it suggests that the motility pattern can improve a microorganism's ability to sequester nutrients in a competitive environment.

INTRODUCTION

Cell motility comes with a big cost. This is the reason its associated genes are tightly regulated (1,2). A high cost is usually accompanied by a high benefit, suggesting that motility is important for cell survival. The ultimate benefit of bacterial motility is that it allows a cell to sequester essential resources more efficiently in a competitive environment. A pelagic ocean is one of those habitats in which the average nutrient level is very low, e.g., the concentration of amino acids is in the range of ~10^{-9} M, and evidence suggests that for small bacteria, the availability of metabolizable carbons is the limiting factor for how fast these bacteria can swim (3). Moreover, in oceans, nutrients appear and disappear in a sporadic fashion, demanding a swift chemical response, a fast swimming speed, and being able to localize near a nutrient patch once it is found. This raises an intriguing question about what motility pattern is better suited for such an environment.

The best studied and characterized bacterial motion is that of the enteric bacterium *Escherichia coli*, which we will call a two-step swimmer. In a homogeneous environment, the cell incorporates a run-tumble swimming pattern to navigate. In an inhomogeneous environment, the cell extends (shortens) its run intervals when it moves up (down) a chemoattractant gradient, leaving the tumbling interval that randomizes the swimming direction relatively unchanged (4). By modulating the run intervals based on chemical cues, the bacterium executes a biased random walk, allowing it to home in on the source of beneficial chemicals and away from harmful ones. However, as far as we know, marine bacteria do not use run-tumble to navigate. Instead, they use the forward-reverse pattern, which has been the most documented in works by Taylor and Koshland (5) and Luchsinger et al. (6). In a study in 2011 (7), we found that marine bacteria *Vibrio alginolyticus*, and possibly others, swims using a cyclic three-step motility pattern, forward-reverse-flick. Specifically, the bacterium swims forward for an interval Δ_{CCW} propelled by a CCW-rotating left-handed polar flagellum, and then swims backward for an interval Δ_{CW} pulled by the CW-rotating flagellum. Upon another motor reversal, which causes the bacterium to swim forward again, the polar flagellum deflects, causing the cell body to reorient in a new random direction. Compared to Δ_{CCW} or Δ_{CW}, which is ~0.5 s, the flick is very brief, lasting ~0.05 s.

Despite the different motility pattern of the marine bacterium, which we will call a three-step swimmer, its trajectory is still a random walk but with a reduced net displacement within a swimming cycle ($\Delta_{CCW}+\Delta_{CW}$) because of the backtracking (7). This raises an interesting question about the benefit for a microorganism to adopt the three-step run-reverse-flick motility pattern instead of the two-step run-tumble pattern. In a more general sense, one may ask whether certain motility patterns are better suited for a given environment than others. These important questions are difficult to address by laboratory experiments because different microorganisms have different swimming speeds, chemical sensitivities, and intrinsic switching rates. Indeed, our previous experiment showed that *V. alginolyticus* can migrate in an attractant gradient much faster than *E. coli*, which may be expected because its swimming speed is 2–3 times greater (7). However, the marine bacteria also form a tighter aggregate at the top of a gradient, which is not evident and appears at odds with its high swimming

Submitted January 28, 2014, and accepted for publication July 24, 2014.

*Correspondence: xlwu@pitt.edu

Editor: Reinhard Lipowsky.

0006-3495/14/10/1712/9 $2.00

http://dx.doi.org/10.1016/j.bpj.2014.07.058

speed. Hence, unless the problem can be analyzed in an objective manner, there will be no satisfactory answer to these questions.

To overcome this impasse, we resort to mathematical modeling using master equations. A swimming bacterium is represented by a random walker obeying specific local dynamics in a chemical gradient. The two-step and three-step swimmers are identical in all aspects except their motility patterns. We found that for a microorganism executing the run-tumble cycles, the master equation is the standard convection-diffusion equation, or, in the biological context, known as the Keller-Segal (KS) equation (8). On the other hand, for a microorganism executing the run-reverse-flick cycles, the master equation is not of the standard form. It contains an extra flux term, which we show to be negligible. A simple but surprising physical picture emerging from our calculation is that a microorganism can alter its microscopic motility pattern to significantly reduce its diffusivity without compromising the drift velocity in a chemical gradient. This suggests that in oceans, the motility pattern such as run-reverse-flick or, for that matter run-reverse, is selected for its localization or exploitative behavior rather than its exploration potential.

This article is organized in the following fashion: To begin, the two-step and three-step motility patterns, which may be viewed as the chemotactic strategies, are implemented at a microscopic level in one spatial dimension. This results in differential equations similar to diffusion equations of the telegraph model (9). By specifying the switching rate $k(x)$ as a function of local chemical concentration $c(x)$, we show that the master equation is equivalent to the KS equation that contains two phenomenological constants, the bacterial diffusivity D and the chemotactic coefficient $\chi = v_d/\nabla c$, where v_d is the drift velocity and ∇c is the chemical gradient. The KS equation is thus a general description of bacterial chemotaxis, and different motility patterns result in different D and χ. Analytic solutions are then obtained approximately for the one-dimensional case and compared with numerical solutions without approximations. Finally, the one-dimensional calculation is generalized to higher spatial dimension d, and we show that our central finding is independent of the spatial dimension.

RESULTS AND DISCUSSIONS

The theoretical models in one dimension

The movement of a bacterium is akin to that of a random walker. The cell swims with a constant velocity for a time Δ and turns to a new random direction, where Δ is exponentially distributed. A model describing a diffusing particle with a finite mass is thus appropriate for mimicking chemotactic behavior of a bacterium. Here, we are only interested in the long-time diffusive regime of particle dynamics. We define the probability density functions (PDFs) of particles moving in the $\hat{x}$ and $-\hat{x}$ directions as $P(\hat{x},x,t)$ and $P(-\hat{x},x,t)$, respectively (9). These particles are subject to random collisions or directional randomization that occur at rates $k_+(x)$ and $k_-(x)$ when moving in the $\hat{x}$ and $-\hat{x}$ directions, respectively. After a collision, the particles have an even chance of continuing in the same or opposite direction. The PDFs are then given by

$$\frac{\partial P(\hat{x},x,t)}{\partial t} = -v\frac{\partial P(\hat{x},x,t)}{\partial x} - \frac{k_+(x)}{2}P(\hat{x},x,t) + \frac{k_-(x)}{2}P(-\hat{x},x,t), \quad (1)$$

$$\frac{\partial P(-\hat{x},x,t)}{\partial t} = v\frac{\partial P(-\hat{x},x,t)}{\partial x} + \frac{k_+(x)}{2}P(\hat{x},x,t) - \frac{k_-(x)}{2}P(-\hat{x},x,t). \quad (2)$$

In a homogeneous medium, the collision rates are expected to be constant, $k_\pm(x) = k_0$, independent of x. However, for chemotaxis, a bacterium follows chemical cues by modulating $k_\pm(x)$: if the bacterium swims up an attractant gradient, it lowers the switching rate, and if it swims down the gradient, it increases the switching rate. This assumption is valid in the case of *V. alginolyticus* (10).

Previous experiments have shown that a bacterium performs chemosensing by temporal comparison. In *E. coli*, for example, the chemoreceptors average the receptor occupancy by chemoeffectors in the present one-second and compare it with that of the previous three seconds (11). The result of the comparison is used to alter the phosphorylation level of the regulator protein CheY that determines the flagellar motor switching probability. In 2011, we found that marine bacteria *V. alginolyticus* also perform temporal comparison, but the response time is shorter (10). Hence, even though bacterial chemotaxis is modeled as a random walk, the actual process is non-Markovian because $k_\pm(x)$ is determined by the history of a particular trajectory (12,13). Because of this memory effect, a rigorous treatment requires averaging over all possible trajectories, which is beyond the scope of this work. The bacterial sensory response can be significantly simplified if the chemoeffector, say an attractant, $c(x)$, has a shallow gradient that does not change much during a swimming interval, $v|\partial^2 c/\partial x^2| \ll k_0\,|\partial c/\partial x|$. In this case, the switching rate is a linear function of the chemical gradient $k_\pm(x) \approx k_0 \mp \Delta k(x)$ (9) with $\Delta k(x) = gv\partial c(x)/\partial x$ and g being a gain factor. In an early work by Mesibov et al. (14), it was shown that instead of linear sensing, bacteria actually use logarithmic sensing to respond to a chemical cue. In this case, $\Delta k(x) = (g'/c(x))v\partial c(x)/\partial x$, where g' is a constant. Work in 2009 showed that $c(x)$ in $g \equiv g'/c(x)$ can be replaced by $\bar{c}$, the average concentration experienced by the bacterium in an attractant profile if $\partial c(x)/\partial x \ll k_0 c(x)/v$ (15).

The master equation for two-step swimmers

For the run-tumble motility pattern in a shallow gradient, Eqs. 1 and 2 can be used directly by replacing $k_\pm$ with $k_0 \mp \Delta k$. This yields

$$\frac{\partial P(\widehat{x},x,t)}{\partial t} = -v\frac{\partial P(\widehat{x},x,t)}{\partial x} - \frac{k_0-\Delta k(x)}{2}P(\widehat{x},x,t) + \frac{k_0+\Delta k(x)}{2}P(-\widehat{x},x,t), \quad (3)$$

$$\frac{\partial P(-\widehat{x},x,t)}{\partial t} = v\frac{\partial P(-\widehat{x},x,t)}{\partial x} + \frac{k_0-\Delta k(x)}{2}P(\widehat{x},x,t) - \frac{k_0+\Delta k(x)}{2}P(-\widehat{x},x,t). \quad (4)$$

Adding and subtracting Eqs. 3 and 4, we obtain

$$\frac{\partial P(x,t)}{\partial t} = -\frac{\partial J(x,t)}{\partial x}, \quad (5)$$

$$\frac{\partial J(x,t)}{\partial t} = -v^2\frac{\partial P(x,t)}{\partial x} - k_0 J(x,t) + v\Delta k(x)P(x,t), \quad (6)$$

where

$$P(x,t) = P(\widehat{x},x,t) + P(-\widehat{x},x,t)$$

is the total probability and

$$J(x,t) = v(P(\widehat{x},x,t) - P(-\widehat{x},x,t))$$

is the flux. Taking the time derivative of Eq. 5 and replacing $\partial J/\partial t$ by Eq. 6 gives

$$\frac{\partial^2 P(x,t)}{\partial t^2} = -\frac{\partial}{\partial x}\left[-v^2\frac{\partial P(x,t)}{\partial x} - k_0 J(x,t) + v\Delta k(x)P(x,t)\right]. \quad (7)$$

Because only the long-time behavior ($k_0 t \gg 1$) of the bacterial population is of interest, it is justifiable to set $\partial^2 P(x,t)/\partial t^2 = 0$. This yields

$$\frac{\partial J(x,t)}{\partial x} = -\frac{v^2}{k_0}\frac{\partial^2 P(x,t)}{\partial x^2} + \frac{v}{k_0}\frac{\partial(\Delta k(x)P(x,t))}{\partial x}. \quad (8)$$

Inserting this equation into Eq. 5, we arrive at the master equation for the two-step swimmer,

$$\frac{\partial P_E(x,t)}{\partial t} + \frac{\partial(v_E(x)P_E(x,t))}{\partial x} = D_E\frac{\partial^2 P_E(x,t)}{\partial x^2}, \quad (9)$$

where the subscript E stands for *E. coli*, $v_E(x) = v\Delta k(x)/k_0$ is the drift velocity, and $D_E = v^2/k_0$ is the diffusivity. We observed that for the two-step swimmer, the master (or KS) equation can be derived with the single assumption $k_0 t \gg 1$. As we shall see, this is insufficient for the three-step swimmer.

The master equation for three-step swimmers

The major difference between a two-step and a three-step swimmer is that the latter has motility even when the flagellar motor rotates in the CW direction, backtracking its forward path. For the three-step swimmer, therefore, there are four possibilities depending on the swimming direction and the state of motor rotation: $(\widehat{x},\mathrm{CCW})$, $(-\widehat{x},\mathrm{CCW})$, $(\widehat{x},\mathrm{CW})$, and $(-\widehat{x},\mathrm{CW})$. The corresponding PDFs evolve in time according to

$$\frac{\partial P_{\mathrm{CCW}}(\widehat{x},x,t)}{\partial t} = -v\frac{\partial P_{\mathrm{CCW}}(\widehat{x},x,t)}{\partial x} - (k_0-\Delta k)P_{\mathrm{CCW}}(\widehat{x},x,t) + \frac{k_0-\Delta k}{2}P_{\mathrm{CW}}(\widehat{x},x,t) + \frac{k_0+\Delta k}{2}P_{\mathrm{CW}}(-\widehat{x},x,t), \quad (10)$$

$$\frac{\partial P_{\mathrm{CCW}}(-\widehat{x},x,t)}{\partial t} = v\frac{\partial P_{\mathrm{CCW}}(-\widehat{x},x,t)}{\partial x} - (k_0+\Delta k)P_{\mathrm{CCW}}(-\widehat{x},x,t) + \frac{k_0-\Delta k}{2}P_{\mathrm{CW}}(\widehat{x},x,t) + \frac{k_0+\Delta k}{2}P_{\mathrm{CW}}(-\widehat{x},x,t), \quad (11)$$

$$\frac{\partial P_{\mathrm{CW}}(\widehat{x},x,t)}{\partial t} = -v\frac{\partial P_{\mathrm{CW}}(\widehat{x},x,t)}{\partial x} - (k_0-\Delta k)P_{\mathrm{CW}}(\widehat{x},x,t) + (k_0+\Delta k)P_{\mathrm{CCW}}(-\widehat{x},x,t), \quad (12)$$

$$\frac{\partial P_{\mathrm{CW}}(-\widehat{x},x,t)}{\partial t} = v\frac{\partial P_{\mathrm{CW}}(-\widehat{x},x,t)}{\partial x} - (k_0+\Delta k)P_{\mathrm{CW}}(-\widehat{x},x,t) + (k_0-\Delta k)P_{\mathrm{CCW}}(\widehat{x},x,t). \quad (13)$$

In the above, the cyclic run-reverse-flick motility pattern is explicitly implemented, i.e., when a bacterium swims in a CCW state, a motor reversal simply makes the cell swim in the opposite direction, but when a bacterium swims in a CW state, a motor reversal causes the cell to flick and swim either in its current or opposite direction with equal probability.

Similar to the two-step case, we define the total probability

$$P(x,t) = P_{\mathrm{CCW}}(\widehat{x},x,t) + P_{\mathrm{CCW}}(-\widehat{x},x,t) + P_{\mathrm{CW}}(\widehat{x},x,t) + P_{\mathrm{CW}}(-\widehat{x},x,t)$$

and the flux

$$J = v(P_{\mathrm{CCW}}(\widehat{x},x,t) + P_{\mathrm{CW}}(\widehat{x},x,t) - P_{\mathrm{CCW}}(-\widehat{x},x,t) - P_{\mathrm{CW}}(-\widehat{x},x,t))$$

for the three-step swimmer. Summing up Eqs. 10–13 yields the equation of conservation of total number of bacteria,

$$\frac{\partial P(x,t)}{\partial t} = -\frac{\partial J(x,t)}{\partial x}, \tag{14}$$

which is expected. However, the flux equation is more complicated with the result

$$\frac{\partial J(x,t)}{\partial t} = -v^2\frac{\partial P(x,t)}{\partial x} - 2k_0 J(x,t) + 2v\Delta k(x)P(x,t) + k_0\delta J_{\mathrm{CW}}(x,t), \tag{15}$$

where

$$\delta J_{\mathrm{CW}}(x,t) \equiv v(P_{\mathrm{CW}}(\widehat{x},x,t) - P_{\mathrm{CW}}(-\widehat{x},x,t)) - \frac{v\Delta k(x)}{k_0}(P_{\mathrm{CW}}(\widehat{x},x,t) + P_{\mathrm{CW}}(-\widehat{x},x,t))$$

is the extra flux term, which makes this equation different from Eq. 6. Following the same procedure as above, i.e., taking the time derivative of Eq. 14 and replacing $\partial J/\partial t$ using Eq. 15, we found in the long-time limit,

$$\frac{\partial P(x,t)}{\partial t} = \frac{v^2}{2k_0}\frac{\partial^2 P(x,t)}{\partial x^2} - \frac{v}{k_0}\frac{\partial(\Delta k(x)P(x,t))}{\partial x} - \frac{1}{2}\frac{\partial\delta J_{\mathrm{CW}}(x,t)}{\partial x}. \tag{16}$$

In the Supporting Material, it is shown that $\delta J_{\mathrm{CW}} \sim o(\Delta k)$ and can be neglected when $\Delta k/k_0 \ll 1$. This is also confirmed by numerical calculations in which all terms are included. Dropping the last term in Eq. 16, we finally obtained the master equation for the three-step swimmer,

$$\frac{\partial P_V(x,t)}{\partial t} + \frac{\partial(v_V(x)P_V(x,t))}{\partial x} = D_V\frac{\partial^2 P_V(x,t)}{\partial x^2}, \tag{17}$$

where the subscript V stands for *V. alginolyticus*, $v_V(x) = v\Delta k(x)/k_0$, and $D_V = v^2/2k_0$. We note that by dropping the $\partial\delta J_{\mathrm{CW}}/\partial x$ term, the master equation for the three-step swimmer is mathematically identical to that of the two-step swimmer. Importantly, we found that the bacterial diffusivity of the three-step swimmer is a factor of two smaller than that of the two-step swimmer, $D_V = D_E/2$, but the drift velocity is the same for both $v_V = v_E = v_d(\equiv v\Delta k/k_0)$; the latter is unexpected because, due to backtracking, one anticipates $v_V < v_E$. The result is in contrast with inanimate particles. For example, for a colloidal particle in an external field, diffusion and drift are related; when one increases, the other must increase, inasmuch as both share the same frictional factor.

The above finding has important biological implications because it shows that by altering the motility pattern, a microorganism can reduce its diffusivity without compromising its drift velocity, a niche that can be exploited by the microorganism. Indeed, Eqs. 9 and 17 provide clues about how well a two-step and three-step swimmer can perform chemotaxis in a chemical gradient. It shows that for everything being equal, such as the swimming speed v, the switching rate k_0, and the gain factor g (or g'), the three-step swimmer can aggregate around a source of an attractant more tightly than its two-step counterpart, allowing a higher exposure to nutrients. Such a trait is very significant for competitive foraging in habitats where nutrients are scarce and localized. The high ability for the cell to localize evidently comes with a cost. It reduces the chance for the three-step swimmer to explore habitats efficiently. However, it may be argued that, in vast oceans, searching is unproductive unless a chemical signal is present. In this case, it is more important to follow closely and rapidly an existing chemical cue. This exploitative behavior appears to be encoded in the swimming pattern of *V. alginolyticus*.

Analytical and numerical solutions of the master equations

It is difficult to obtain analytical solutions to the master equation with an arbitrary drift velocity $v_d(x)$. However, when the chemical gradient is linear, Δk and v_d become constant and the problem is simplified. Below we attempt to find analytical solutions in the domain $[-L, L]$ with different initial conditions when an chemoattractant concentration increases linearly along x. Using the method of separation of variables, we found that the solution to the master equation is given by

$$P(x,t) = \frac{q'}{\sinh(2q'L)}\exp(2q'x) + \exp(q'x) \times \left[\sum_{n=1,2,..} A_n\psi_n(x)\exp(-\lambda_n t) + \sum_{m=0,1,2,..} B_m\phi_m(x)\exp(-\lambda_m t)\right], \tag{18}$$

where $q' = v_d/2D$ is the wavenumber characterizing the steady-state profile, $\psi_n(x)$ and $\phi_m(x)$ are the eigenfunctions, and λ_n and λ_m are the corresponding decay rates. In terms of wavenumbers

$$q_n = \frac{\pi n}{L} \text{ and } q_m = \frac{\pi(2m+1)}{2L},$$

they are given by

$$\begin{cases} \psi_n(x) = \psi_{0n}(q_n \cos(q_n x) + q' \sin(q_n x)) \\ \phi_m(x) = \phi_{0m}(q' \cos(q_m x) - q_m \sin(q_m x)) \end{cases}, \tag{19}$$

$$\begin{cases} \lambda_n = \lambda_0 \left[1 + \left(\frac{q_n}{q'}\right)^2\right], \\ \lambda_m = \lambda_0 \left[1 + \left(\frac{q_m}{q'}\right)^2\right], \end{cases} \tag{20}$$

where

$$\lambda_0 = \frac{v_d^2}{4D},$$

$$\psi_{0n} = \frac{1}{\sqrt{L\left(q'^2 + q_n^2\right)}}, \text{ and}$$

$$\phi_{0m} = \frac{1}{\sqrt{L\left(q'^2 + q_m^2\right)}},$$

and m and n are positive integers.

Consider the situation when the bacteria are released at $x = 0$, and we watch how they spread in space and time. The initial condition in this case is $P(x,0) = \delta(x)$, and it yields the Fourier amplitudes $A_n = \psi_n(0)$ and $B_m = \phi_m(0)$. Fig. 1 displays our analytical solutions of $P(x,t)$ for the two-step (*blue lines*) and three-step (*purple lines*) swimmers, and the results are compared with the numerical solutions (*green squares* and *red circles*, respectively) using the full equations, Eqs. 3 and 4 and Eqs. 10–13. Because of the approximations made in deriving Eqs. 9 and 17, specifically $\partial^2 P/\partial t^2 \simeq 0$ and $\delta J_{\mathrm{CW}} \simeq 0$, the numerical method provides a quantitative means to check their validity. In all numerical calculations, we set $\Delta x = 0.1$ and $\Delta t = 1$ so that the bacterial swimming speed is $v = \Delta x/\Delta t = 0.1$, the switching rate is $k_0 = 0.1/\Delta t$ (or the mean swimming

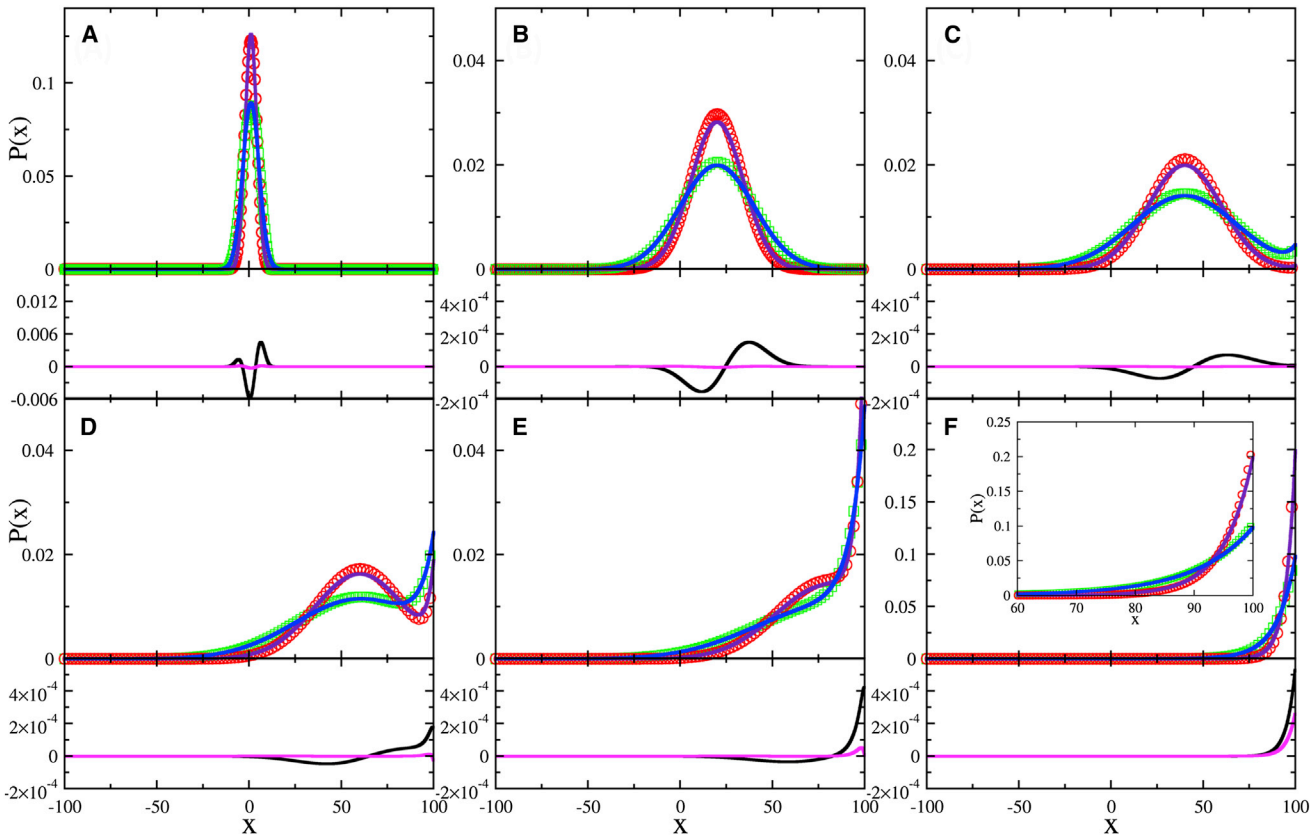

FIGURE 1 Evolution of $P(x,t)$ starting from the δ-distribution $P(x,0) = \delta(x)$. The bacterial profiles of the two-step (*blue line*) and three-step (*purple line*) swimmers, calculated based on Eq. 18 at reduced times $t/t_v = 0.01$, 0.2, 0.4, 0.6, 0.8, and 2, are plotted in panels *A–F*, respectively. Here the chemoattractant concentration increases linearly along x, t_v ($\equiv L/v_d$) $10^4\Delta t$, and $\Delta t = 1$ is the computation step. As seen, the steady-state exponential profiles are formed at $t/t_v \simeq 2$. (*Green squares* and *red circles*) Numerical solutions for Eqs. 3 and 4, and 10–13, respectively. (*F, inset*) Close-up for the steady-state profiles, where colored symbol and line designations are the same as above. Beneath each PDF, the first two terms $(v^2/2k_0)(\partial^2 P/\partial x^2) - v(\Delta k/k_0)(\partial P/\partial x)$ (*black lines*) and the last term $1/2(\partial/\partial x)\delta J_{\mathrm{cw}}$ (*magenta lines*) on the right-hand side of Eq. 16 are plotted based on the numerical solutions. As seen, the extra flux term is significant only for late times. However, the analytic calculation without this term still yields a quantitatively good result, as demonstrated in panel *F* (*inset*). To see this figure in color, go online.

interval $k_0^{-1} = 10\Delta t$), and the change in switching rate is $\Delta k = k_0/10$.

One observes that for the two-step swimmer, the analytical and numerical solutions are nearly identical, indicating that the short-time, ballistic-like motion of bacteria does not contribute significantly to the evolution of the bacterial profile. For the three-step swimmer, on the other hand, small discrepancies can be seen at the peak of bacterial profiles, indicating that in this region the extra flux term, $\partial\delta J_{CW}/\partial x$, in Eq. 16 has a small but discernible contribution. However, the overall good agreement between the analytic and the numerical solutions demonstrates that 1), our derivation of the master equations is sound, and 2), the approximations are reasonable.

It is noteworthy that the numerical solutions support our analysis that the microscopic motility patterns do not affect the drift velocity v_d. They only modify the bacterial diffusivity D. This is illustrated by Fig. 1, which shows that the two bacteria migrate up the chemical gradient with identical speed, but the bacterial pack for the three-step swimmer is narrower than its two-step counterpart. Our calculations also show that because of the spatial separation between the chemical source ($x = L$) and the initial bacterial position ($x = 0$), a waiting time of $t_v \sim L/v_d$ is required for the bacteria to aggregate around the top of the attractant concentration. As delineated by Fig. 1 *F*, the steady state is reached when $t/t_v \simeq 2$.

For a better comparison with experimental measurements, we also calculated evolution of bacterial profiles starting from a uniform distribution, $P(x,0) = 1/2L$. The result of this calculation and the accompanied discussion are included in the Supporting Material.

Comparison of nutrient exposure to two-step and three-step swimmers

Biologically it is useful to quantify nutrient exposure due to different motility patterns because this quantity is closely related to the fitness of the bacteria (16). In the steady state, the nutrient exposure can be calculated by the overlapping integral between the bacterial distribution $P(x)$ and the attractant distribution $c(x)$. For simplicity, we assumed that the nutrient is confined in the domain $[-L, L]$ and has an exponential profile

$$c(x) = c(L)\exp((x-L)/l),$$

where $c(L)$ is the attractant concentration at $x = L$ and l is the decay length. The linear gradient is the special case when $l \gg L$. In the steady state, the bacterial profile $P(x)$ satisfies the equation

$$D\frac{\partial P(x)}{\partial x} - v_d(x)P(x) = 0, \qquad (21)$$

where

$$v_d(x) = \frac{gv^2}{k_0}\frac{\partial c}{\partial x}$$

and the gain factor g is assumed to be a constant. Solving Eq. 21 and using the general expression $D = v^2/\varepsilon k_0$, we found

$$P(x) = P(L)\exp\left[\epsilon gc(L)\left(\exp\left(\frac{x-L}{l}\right) - 1\right)\right],$$

where $\varepsilon = 1$ and 2 correspond to two-step and three-step swimmers, respectively. It follows that the average nutrient exposure per bacterium is given by

$$C = \int_{-L}^{L} P(x)c(x)dx \Big/ \int_{-L}^{L} P(x)dx.$$

This allows us to compute the ratio of the nutrient exposure C_V/C_E of the two bacteria,

$$\frac{C_V}{C_E} = \frac{\int_{-2L}^{0}\exp[2gc(L)(\exp(x/l)-1)]\exp(x/l)dx}{\int_{-2L}^{0}\exp[gc(L)(\exp(x/l)-1)]\exp(x/l)dx} \times \frac{\int_{-2L}^{0}\exp[gc(L)(\exp(x/l)-1)]dx}{\int_{-2L}^{0}\exp[2gc(L)(\exp(x/l)-1)]dx}.$$

The above expression was numerically integrated, and the result is presented in Fig. 2. As can be seen, the advantage of the three-step motility pattern over the two-step pattern

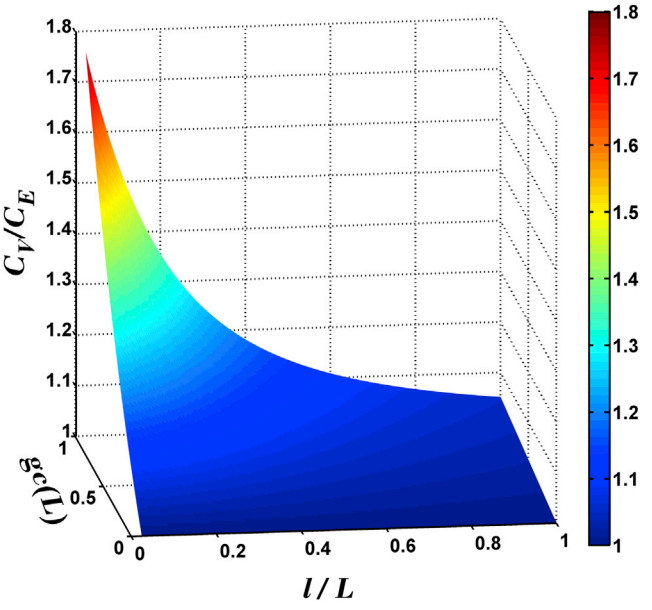

FIGURE 2 The ratio of nutrient exposure C_V/C_E versus l/L and $gc(L)$. Here C_V (C_E) is the average nutrient exposure when the three-step (two-step) swimmers are exposed to exponentially distributed chemoattractant in a box of size $2L$. The advantage of three-step over two-step swimming becomes more significant when the scale of the chemical distribution, l, is small compared to the size of the box L and the bacteria have a large gain factor g. To see this figure in color, go online.

is significant only when $gc(L)$ is large and l/L is small. For a shallow gradient $l/L \gg 1$, the improvement

$$\Delta C/C_E\left(\equiv\frac{C_V - C_E}{C_E}\right)$$

is only a few percent in the best case. This result suggests that the three-step motility pattern is better suited for a localized source, and to benefit from such a strategy, the cell must have a large gain g.

Master equations in high spatial dimensions

It is possible to generalize the one-dimensional calculations to higher spatial dimensions d (9). Let $\hat{u}$ be a unit vector specifying the swimming direction of a bacterium. We define two subpopulations $P_{\mathrm{CCW}}(\hat{u},x,t)$ and $P_{\mathrm{CW}}(\hat{u},x,t)$ based on their motor directions. These two populations evolve according to

$$\begin{aligned}\frac{\partial P_{\mathrm{CCW}}(\hat{u},x,t)}{\partial t} &= -v\vec{\nabla}\cdot(\hat{u}P_{\mathrm{CCW}}(\hat{u},x,t))\\ &\quad - k(x,\hat{u})P_{\mathrm{CCW}}(\hat{u},x,t)\\ &\quad + \int k(x,\hat{u}')P_{\mathrm{CW}}(\hat{u}',x,t)W(\hat{u},\hat{u}')d\Omega_{\hat{u}'},\end{aligned} \tag{22}$$

$$\begin{aligned}\frac{\partial P_{\mathrm{CW}}(\hat{u},x,t)}{\partial t} &= -v\vec{\nabla}\cdot(\hat{u}P_{\mathrm{CW}}(\hat{u},x,t))\\ &\quad - k(x,\hat{u})P_{\mathrm{CW}}(\hat{u},x,t)\\ &\quad + \int k(x,\hat{u}')P_{\mathrm{CCW}}(\hat{u}',x,t)W'(\hat{u},\hat{u}')d\Omega_{\hat{u}'},\end{aligned} \tag{23}$$

where $k(x,\hat{u})$ is the switching rate, which is assumed to be identical for both CCW and CW intervals; $W(\hat{u},\hat{u}')$ ($W'(\hat{u},\hat{u}')$) is the probability that upon a motor reversal from CW (CCW) to CCW (CW), the bacterium changes swimming direction from $\hat{u}'$ to $\hat{u}$; and $d\Omega_{\hat{u}'}$ indicates integration over the solid angle spanned by $\hat{u}'$. For a bacterium that executes a run-reverse-flick motility pattern, $W'(\hat{u},\hat{u}') = \delta_{\hat{u},-\hat{u}'}$ so that $W'(\hat{u},\hat{u}') = 1$ if $\hat{u} = -\hat{u}'$ and otherwise $W'(\hat{u},\hat{u}') = 0$. Moreover, if $\hat{u}$ and $\hat{u}'$ are uncorrelated, i.e., when a flick completely randomizes the swimming direction which is approximately valid for *V. alginolyticus* (7), $W(\hat{u},\hat{u}') = \Omega_d^{-1}$, where

$$\Omega_d\left(\equiv\int d\Omega_{\hat{u}'}\right) = 2\pi$$

for $d = 2$ and $\Omega_d = 4\pi$ for $d = 3$.

Following the one-dimensional derivation, we define

$$P_{\mathrm{CCW}}(x,t)\equiv\int P_{\mathrm{CCW}}(\hat{u},x,t)d\Omega_{\hat{u}},$$

$$P_{\mathrm{CW}}(x,t)\equiv\int P_{\mathrm{CW}}(\hat{u},x,t)d\Omega_{\hat{u}},$$

$$\vec{J}_{\mathrm{CCW}}(x,t)\equiv v\int P_{\mathrm{CCW}}(\hat{u},x,t)\hat{u}d\Omega_{\hat{u}},\ \text{and}$$

$$\vec{J}_{\mathrm{CW}}(x,t)\equiv v\int P_{\mathrm{CW}}(\hat{u},x,t)\hat{u}d\Omega_{\hat{u}}.$$

The total probability density function $P(x,t)$ and the total current $\vec{J}(x,t)$ are then given by $P(x,t) \equiv P_{\mathrm{CCW}}(x,t) + P_{\mathrm{CW}}(x,t)$ and $\vec{J}(x,t)\equiv\vec{J}_{\mathrm{CCW}}(x,t)+\vec{J}_{\mathrm{CW}}(x,t)$. By adding Eqs. 22 and 23 and integrating both sides over all possible directions $\hat{u}$, we find

$$\frac{\partial P(x,t)}{\partial t} = -\vec{\nabla}\cdot\vec{J}(x,t). \tag{24}$$

To compute $\vec{J}_{\mathrm{CCW}}(x,t)$, multiply both sides of Eqs. 22 by $v\hat{u}$, and integrate over $\hat{u}$. Because

$$\int W(\hat{u},\hat{u}')\hat{u}d\Omega_{\hat{u}} = 0,$$

we have

$$\begin{aligned}\frac{\partial\vec{J}_{\mathrm{CCW}}(x,t)}{\partial t} &= -v^2\int\hat{u}\vec{\nabla}\cdot(\hat{u}P_{\mathrm{CCW}}(\hat{u},x,t))d\Omega_{\hat{u}}\\ &\quad - v\int\hat{u}k(x,\hat{u})P_{\mathrm{CCW}}(\hat{u},x,t)d\Omega_{\hat{u}}.\end{aligned} \tag{25}$$

Likewise, using Eq. 23, we obtain

$$\begin{aligned}\frac{\partial\vec{J}_{\mathrm{CW}}(x,t)}{\partial t} &= -v^2\int\hat{u}\vec{\nabla}\cdot(\hat{u}P_{\mathrm{CW}}(\hat{u},x,t))d\Omega_{\hat{u}}\\ &\quad - v\int\hat{u}k(x,\hat{u})(P_{\mathrm{CW}}(\hat{u},x,t)\\ &\quad + P_{\mathrm{CCW}}(\hat{u},x,t))d\Omega_{\hat{u}}.\end{aligned} \tag{26}$$

Adding Eqs. 25 and 26 results in

$$\begin{aligned}\frac{\partial\vec{J}(x,t)}{\partial t} &= -v^2\int\hat{u}\vec{\nabla}\cdot(\hat{u}P(\hat{u},x,t))d\Omega_{\hat{u}}\\ &\quad -2v\int\hat{u}k(x,\hat{u})P(\hat{u},x,t)d\Omega_{\hat{u}}\\ &\quad + v\int\hat{u}k(x,\hat{u})P_{\mathrm{CW}}(\hat{u},x,t)d\Omega_{\hat{u}}.\end{aligned} \tag{27}$$

For shallow chemoattractant gradients, the switching rate is expanded about the steady-state value k_0, resulting in

$$k(x,\hat{u}) \approx k_0 - \Delta k(x,\hat{u})$$

where $\Delta k(x,\hat{u}) = gv\hat{u}\cdot\vec{\nabla}c(x)$. The equation of motion for the current becomes

$$\frac{\partial \vec{J}(x,t)}{\partial t} = -v^2\int \hat{u}\vec{\nabla}\cdot(\hat{u}P(\hat{u},x,t))d\Omega_{\hat{u}} - 2k_0\vec{J}(x,t) + 2v\int \hat{u}\Delta k(x,\hat{u})P(\hat{u},x,t)d\Omega_{\hat{u}} + k_0\delta\vec{J}_{\mathrm{CW}}(x,t), \tag{28}$$

where the extra flux term is given by

$$\delta\vec{J}_{\mathrm{CW}}(x,t) = \vec{J}_{\mathrm{CW}}(x,t) - \frac{v}{k_0}\int \hat{u}\Delta k(x,\hat{u})P_{\mathrm{CW}}(\hat{u},x,t)d\Omega_{\hat{u}}.$$

This term originates from the flicking step in the CW interval (see the last term on the right-hand-side of Eq. 22), and directional randomization accounts for its smallness compared to the flux term in the CCW interval. Taking an additional time derivative on both sides of Eq. 24, plugging in Eq. 28, and dropping both $\partial^2 P/\partial t^2$ and $\delta\vec{J}(x,t)$ terms, we arrive at the master equation for d dimensions:

$$\frac{\partial P_V(x,t)}{\partial t} = \frac{v^2}{2k_0}\vec{\nabla}\cdot\left[\int \hat{u}\vec{\nabla}\cdot(\hat{u}P_V(\hat{u},x,t))d\Omega_{\hat{u}}\right] - \frac{v}{k_0}\vec{\nabla}\cdot\left[\int \hat{u}\Delta k(x,\hat{u})P_V(\hat{u},x,t)d\Omega_{\hat{u}}\right]. \tag{29}$$

Equation 29 should be compared with the master equation for the two-step swimmers, which has been derived in the work by Schnitzer (9) as

$$\frac{\partial P_E(x,t)}{\partial t} = \frac{v^2}{k_0}\vec{\nabla}\cdot\left[\int \hat{u}\vec{\nabla}\cdot(\hat{u}P_E(\hat{u},x,t))d\Omega_{\hat{u}}\right] - \frac{v}{k_0}\vec{\nabla}\cdot\left[\int \hat{u}\Delta k(x,\hat{u})P_E(\hat{u},x,t)d\Omega_{\hat{u}}\right]. \tag{30}$$

Using the near-equilibrium assumption of Schnitzer (9), which amounts to

$$\left|\vec{J}(x,t)\right| \ll vP(x,t),$$

the distribution $P(\hat{u},x,t)$ is nearly independent of the swimming direction $\hat{u}$, $P(\hat{u},x,t) \approx P(x,t)/\Omega_d$, so that Eqs. 29 and 30 can be written as

$$\frac{\partial P_V(x,t)}{\partial t} = \frac{v^2}{2dk_0}\nabla^2 P_V - \frac{v^2 g}{dk_0}\vec{\nabla}\cdot\left(\vec{\nabla}c(x)P_V\right), \tag{31}$$

and

$$\frac{\partial P_E(x,t)}{\partial t} = \frac{v^2}{dk_0}\nabla^2 P_E - \frac{v^2 g}{dk_0}\vec{\nabla}\cdot\left(\vec{\nabla}c(x)P_E\right), \tag{32}$$

where we have used the mathematical identity

$$\int \hat{u}_i\hat{u}_j d\Omega_{\hat{u}} = \delta_{ij}\Omega_d/d.$$

These equations define the bacterial drift velocity and diffusivity with the results

$$\vec{v}_d \equiv v^2 g\vec{\nabla}c/(dk_0) \text{ and}$$

$$D = v^2/(\epsilon dk_0),$$

where $\varepsilon = 1$ for a two-step swimmer and $\epsilon = 2$ for a three-step swimmer. It is seen, therefore, that the central result obtained in one dimension remains valid in higher spatial dimensions d.

CONCLUSION

The main point of this article is the demonstration that a microorganism can modify its motility pattern at microscopic scales to significantly reduce its diffusivity without compromising its drift velocity in a chemical gradient. This counterintuitive effect results from the fact that, for a two-step swimmer, it "hedges its bet" for each swimming cycle, and on average it moves up the chemical gradient by a distance

$$\frac{1}{2}\left(\frac{v}{k_0-\Delta k} - \frac{v}{k_0+\Delta k}\right) \simeq v\Delta k/k_0^2$$

during the time k_0^{-1}, resulting in the drifting velocity $v_E = v\Delta k/k_0$. Despite the fact that a three-step swimmer also hedges its bet for each swimming cycle, the forward and backward intervals are compensatory. The cell migrates up the gradient by a distance

$$\frac{v}{k_0-\Delta k} - \frac{v}{k_0+\Delta k} \simeq 2v\Delta k/k_0^2$$

during the time $2k_0^{-1}$, yielding the same drifting velocity $v_V = v\Delta k/k_0$. In this regard, the three-step motility pattern can be exploited by microorganisms to improve their fitness in an environment where nutrients exist in small and sparse patches. Earlier observations that marine bacteria *V. alginolyticus* (7), and possibly *Pseudoalteromonas haloplanktis* as well (16), can form a tighter cluster around a small chemical source more rapidly than their *E. coli* counterpart is consistent with such a scenario.

The study of chemotaxis ability of a bacterium cannot be disconnected from its natural habitat, which is characterized by its chemical compositions, concentrations, and distributions of individual components. Bacteria developed different niches to explore and exploit these features. Our model makes specific predictions about how macroscopic chemotaxis behaviors of a microorganism depend on niches such as microscopic motility pattern, swimming speed, and

chemical sensitivity, which are characterized by ε, v, and $\Delta k/k_0$, respectively. This permits a quantitative and objective comparison of chemotaxis abilities of different microorganisms. Issues that are of biological and ecological significance, and can be quantified based on our calculation, include the following:

1. Dynamic evolution of bacterial profiles in the presence of different chemical distributions,
2. The ability to localize or disperse near a small source of attractant or repellent, and
3. The dynamic range and sensitivity in sensing a chemical.

The comparative study can give us a glimpse of the characteristics of the environment that the microorganism inhabits.

Finally, it should be pointed out that the minimal model presented here has not addressed the issues of memory and nonexponential run-time distribution in bacterial chemotaxis; the latter was observed in *V. alginolyticus* (7,17). Physically, bacterial memory is a result of signal transduction in the chemotaxis network and causes a delay in sensing the chemical gradient. Such a delay in general reduces the drift velocity of the cell, inasmuch as after a swimming direction reversal the memory inherited from the previous swimming interval is always in conflict with the gradient experienced by the cell at the presented interval (18). This increases the chance of the bacterium to move in a wrong direction, resulting in a reduced drift velocity. To minimize such an effect, it is necessary to diminish the delay in sensing the chemical gradient. In our minimal model, it is assumed that the cell modulates its switching rate according to the local chemical gradient, which corresponds to the limiting case where there is no delay in computing dc/dt or dc/dx.

As shown in the Supporting Material using the formula developed by de Gennes (17), when the signal processing time is much shorter than the intrinsic run time k_0^{-1} of the microorganism so that the delay in computing dc/dt can be ignored, the drift velocity of the two-step swimmer is the same as that of the three-step swimmer, consistent with the outcome of the minimal model. In contrast, if the delay time is comparable to k_0^{-1}, the drift velocity of the three-step swimmer is cut by half compared to that of the two-step swimmer, as shown in Taktikos et al. (19). At present we do not know the significance of the memory effect and nonexponential run-time distribution in real microorganisms, but these effects can be assessed by comparing experiments with the minimal model. Thus, high-quality measurements specifically designed to test our model is urgently called for.

SUPPORTING MATERIAL

One figure, twelve equations, and supplemental information are available at http://www.biophysj.org/biophysj/supplemental/S0006-3495(14)00806-6.

We thank D. Boyanovsky, D. Jasnow, and C. Yeung for helpful discussions.

The work was supported by the National Science Foundation under grant No. DMR-1305006.

SUPPORTING CITATIONS

References (20,21) appear in the Supporting Material.

REFERENCES

1. Macnab, R. M. 2003. How bacteria assemble flagella. *Annu. Rev. Microbiol.* 57:77–100.
2. Kalir, S., J. McClure, …, U. Alon. 2001. Ordering genes in a flagella pathway by analysis of expression kinetics from living bacteria. *Science.* 292:2080–2083.
3. Mitchell, J. G. 2002. The energetics and scaling of search strategies in bacteria. *Am. Nat.* 160:727–740.
4. Berg, H. C., and D. A. Brown. 1972. Chemotaxis in *Escherichia coli* analysed by three-dimensional tracking. *Nature.* 239:500–504.
5. Taylor, B. L., and D. E. Koshland, Jr. 1974. Reversal of flagellar rotation in monotrichous and peritrichous bacteria: generation of changes in direction. *J. Bacteriol.* 119:640–642.
6. Luchsinger, R. H., B. Bergersen, and J. G. Mitchell. 1999. Bacterial swimming strategies and turbulence. *Biophys. J.* 77:2377–2386.
7. Xie, L., T. Altindal, …, X.-L. Wu. 2011. Bacterial flagellum as a propeller and as a rudder for efficient chemotaxis. *Proc. Natl. Acad. Sci. USA.* 108:2246–2251.
8. Keller, E. F., and L. A. Segel. 1971. Model for chemotaxis. *J. Theor. Biol.* 30:225–234.
9. Schnitzer, M. J. 1993. Theory of continuum random walks and application to chemotaxis. *Phys. Rev. E Stat. Phys. Plasmas Fluids Relat. Interdiscip. Topics.* 48:2553–2568.
10. Altindal, T., S. Chattopadhyay, and X.-L. Wu. 2011. Bacterial chemotaxis in an optical trap. *PLoS ONE.* 6:e18231.
11. Segall, J. E., S. M. Block, and H. C. Berg. 1986. Temporal comparisons in bacterial chemotaxis. *Proc. Natl. Acad. Sci. USA.* 83:8987–8991.
12. Erban, R., and H. G. Othmer. 2006. From individual to collective behavior in bacterial chemotaxis. *SIAM J. Appl. Math.* 65:361–391.
13. Celani, A., and M. Vergassola. 2010. Bacterial strategies for chemotaxis response. *Proc. Natl. Acad. Sci. USA.* 107:1391–1396.
14. Mesibov, R., G. W. Ordal, and J. Adler. 1973. The range of attractant concentrations for bacterial chemotaxis and the threshold and size of response over this range. Weber law and related phenomena. *J. Gen. Physiol.* 62:203–223.
15. Kalinin, Y. V., L. Jiang, …, M. Wu. 2009. Logarithmic sensing in *Escherichia coli* bacterial chemotaxis. *Biophys. J.* 96:2439–2448.
16. Stocker, R., J. R. Seymour, …, M. F. Polz. 2008. Rapid chemotactic response enables marine bacteria to exploit ephemeral microscale nutrient patches. *Proc. Natl. Acad. Sci. USA.* 105:4209–4214.
17. de Gennes, P. G. 2004. Chemotaxis: the role of internal delays. *Eur. Biophys. J.* 33:691–693.
18. Altindal, T., L. Xie, and X.-L. Wu. 2011. Implications of three-step swimming patterns in bacterial chemotaxis. *Biophys. J.* 100:32–41.
19. Taktikos, J., H. Stark, and V. Zaburdaev. 2013. How the motility pattern of bacteria affects their dispersal and chemotaxis. *PLoS ONE.* 8:e81936.
20. Tu, Y., T. S. Shimizu, and H. C. Berg. 2008. Modeling the chemotactic response of *Escherichia coli* to time-varying stimuli. *Proc. Natl. Acad. Sci. USA.* 105:14855–14860.
21. Celani, A., T. Shimizu, and M. Vergassola. 2011. Molecular and functional aspects of bacterial chemotaxis. *J. Stat. Phys.* 144:219–240.

Supporting Material

Long-Time Bacterial Diffusivity of a 3-Step Swimmer

Here we provide an alternative derivation of bacterial diffusivity for 3-step swimmers. Let the bacterium displacement per swimming cycle ($\Delta_{CCW}+\Delta_{CW}$) be $\vec{r}_i$. The total displacement after N cycles is simply $\vec{R}_N = \sum \vec{r}_i$. If there is no directional correlation between $\vec{r}_i$'s, the mean square displacement is given by $\langle \vec{R}_N \cdot \vec{R}_N \rangle = Na^2$, where $a^2 \equiv \langle |\vec{r}_i|^2 \rangle$. This is a general result applicable to 2-step as well as 3-step swimmers. For the 2-step swimmer, the motility is produced only during the CCW intervals and hence $a^2 = v^2 \langle \Delta_{CCW}^2 \rangle = 2v^2 \tau_{CCW}^2$, where $\tau_{CCW} = \langle \Delta_{CCW} \rangle$ and the PDF $P(\Delta_{CCW})$ is exponential. For the 3-step swimmer, both forward and backward intervals produce motility and hence the mean square displacement during one cycle is given by $a^2 = v^2 \langle \delta^2 \rangle$, where $\delta = |\Delta_{CCW} - \Delta_{CW}|$. If both Δ_{CCW} and Δ_{CW} are exponentially distributed, $\langle \Delta_{CCW} \rangle = \tau_{CCW}$ and $\langle \Delta_{CW} \rangle = \tau_{CW}$, and if there is no correlation between Δ_{CCW} and Δ_{CW} in a swimming cycle, the PDF of δ is

$$P(\delta) = \frac{1}{\tau_{CCW} + \tau_{CW}} \left[\exp\left(-\frac{\delta}{\tau_{CCW}} \right) + \exp\left(-\frac{\delta}{\tau_{CW}} \right) \right]. \tag{S1}$$

Below we make the simplifying assumption $\tau_{CCW} \approx \tau_{CW}$, which yields $a^2 = 2v^2 \tau_{CCW}^2$. To complete the calculation, we notices that $N \approx t/\langle \Delta_{CCW} \rangle = t/\tau_{CCW}$ for 2-step swimmers and $N = t/\left(\langle \Delta_{CCW} \rangle + \langle \Delta_{CW} \rangle \right) = t/(2\tau_{CCW})$ for 3-step swimmers, where t is the swimming

time. In d-dimensional space, the bacterial diffusivity D is defined as,

$$\langle \vec{R}_N \cdot \vec{R}_N \rangle = 2dDt, \tag{S2}$$

which gives rise to $D = v^2\tau_{CCW}/d$ for the 2-step swimmers and $D = v^2\tau_{CCW}/(2d)$ for the 3-step swimmers. In one dimension, $d = 1$, the result is consistent with what we derived for the master equations using $\delta J_{CW} = 0$. However, if we use the alternative sorting, assuming $\delta J_{CCW} = 0$, the bacterial diffusivity D is inconsistent with the above calculation.

Conditions of Detailed Balance in the Moving Frame of Swimming Bacteria

In the moving frame of bacteria, the steady state condition requires $\frac{d}{dt}... \equiv (\frac{\partial}{\partial t} \pm v \cdot \frac{\partial}{\partial x})... = 0$. It follows from Eqs. 10-13 in the main text that the following conditions must be satisfied: $P_{CW}(\hat{x}, x, t) = P_{CCW}(\hat{x}, x, t)$, $P_{CCW}(-\hat{x}, x, t) = \frac{k_0 - \Delta k}{k_0 + \Delta k} P_{CCW}(\hat{x}, x, t)$, and $P_{CW}(-\hat{x}, x, t) = \frac{k_0 - \Delta k}{k_0 + \Delta k} P_{CCW}(\hat{x}, x, t)$. This yields $P_{CW}(x, t)\,(\equiv P_{CW}(\hat{x}, x, t) + P_{CW}(-\hat{x}, x, t)) = \frac{2k_0}{k_0 + \Delta k} P_{CCW}(\hat{x}, x, t)$ and $\Delta P_{CW}(x, t)\,(\equiv P_{CW}(\hat{x}, x, t) - P_{CW}(-\hat{x}, x, t)) = \frac{2\Delta k}{k_0 + \Delta k} P_{CCW}(+\hat{x}, x, t)$. The above relations show (i) $J_{CW}\,(\equiv v\Delta P_{CW}) \propto \Delta k$ and (ii) $\delta J_{CW} = J_{CW} - v\frac{\Delta k}{k_0} P_{CW}$ vanishes faster than Δk. Physically, δJ_{CW} is a measure of the deviation from detail balance, and when $\Delta k / k_0 \ll 1$, it can be ignored.

The Discretized Versions of the Master Equations and Their Numerical Solutions

Discretized versions of of the master equations for the 2-step and 3-step swimmer are developed below, and they are used for the numerical calculations. In the continuum limit these equations are consistent with those in the main text, Eqs. 3-4 and Eqs. 10-13. All of our

computations were done with Matlab (The MathWorks).

We divided space into segments of equal size Δx located at $\{x_i\}$, and divided time into equal intervals Δt at $\{t_i\}$. For the 2-step case, the conservation of probability demands,

$$\begin{aligned} P(\hat{x}, x_i, t_i) =& P(\hat{x}, x_{i-1}, t_{i-1}) - \frac{1}{2}\left(k_0 - \Delta k(x_i)\right)\Delta t P(\hat{x}, x_{i-1}, t_{i-1}) \\ &+ \frac{1}{2}\left(k_0 + \Delta k(x_i)\right)\Delta t P(-\hat{x}, x_{i+1}, t_{i-1}) \end{aligned}, \tag{S3}$$

$$\begin{aligned} P(-\hat{x}, x_i, t_i) =& P(-\hat{x}, x_{i+1}, t_{i-1}) - \frac{1}{2}\left(k_0 + \Delta k(x_i)\right)\Delta t P(-\hat{x}, x_{i+1}, t_{i-1}) \\ &+ \frac{1}{2}\left(k_0 - \Delta k(x_i)\right)\Delta t P(\hat{x}, x_{i-1}, t_{i-1}) \end{aligned}. \tag{S4}$$

Physically, $P(\hat{x}, x_i, t_i)$ (or $P(-\hat{x}, x_i, t_i)$) is the probability of finding a cell swimming in $\hat{x}$ (or $-\hat{x}$) direction at x_i and t_i. If a cell reaches x_i at time t_i, it must be either at x_{i-1} swimming along the $\hat{x}$ direction or at x_{i+1} swimming along the $-\hat{x}$ direction at time t_{i-1}. Among cells arriving from x_{i-1}, which is $P(\hat{x}, x_{i-1}, t_{i-1})$, $1 - (k_0 - \Delta k(x_i))\Delta t$ of them will continue in the current swimming direction $\hat{x}$, and $(k_0 - \Delta k(x_i))\Delta t$ of them will randomize their swimming direction. Upon direction randomization, 50% of the this sub-population swims in $\hat{x}$ and the other 50% in $-\hat{x}$ direction. Together, $1 - \frac{1}{2}(k_0 - \Delta k(x_i))\Delta t$ of $P(\hat{x}, x_{i-1}, t_{i-1})$ contributes to $P(\hat{x}, x_i, t_i)$, which corresponds to the first two terms in Eq. S3. Likewise, the same argument shows that $\frac{1}{2}(k_0 + \Delta k(x_i))\Delta t$ of $P(-\hat{x}, x_{i+1}, t_{i-1})$ also contributes to $P(\hat{x}, x_i, t_i)$, which corresponds to the last term in Eq. S3. Similar conservation equations can be derived for the sub-population $P(-\hat{x}, x_i, t_i)$, yielding Eq. S4. Expanding terms in the above equations around x_i and t_i, we recovered the continuous master equations, Eqs. 3-4, in the limits $\Delta x \to 0$, $\Delta t \to 0$, and $\Delta x/\Delta t \to v$.

The derivation for the 3-step case is more tedious, but the idea is the same. The four

equations are given by,

$$\begin{aligned} P_{CCW}(\hat{x}, x_i, t_i) = [1 - (k_0 - \Delta k(x_i))\,\Delta t] P_{CCW}(\hat{x}, x_{i-1}, t_{i-1}) \\ + \frac{1}{2}(k_0 - \Delta k(x_i))\,\Delta t P_{CW}(\hat{x}, x_{i-1}, t_{i-1}) \\ + \frac{1}{2}(k_0 + \Delta k(x_i))\,\Delta t P_{CW}(-\hat{x}, x_{i+1}, t_{i-1}) \end{aligned} \quad , \tag{S5}$$

$$\begin{aligned} P_{CCW}(-\hat{x}, x_i, t_i) = [1 - (k_0 + \Delta k(x_i))\,\Delta t] P_{CCW}(-\hat{x}, x_{i+1}, t_{i-1}) \\ + \frac{1}{2}(k_0 + \Delta k(x_i))\,\Delta t P_{CW}(-\hat{x}, x_{i+1}, t_{i-1}), \\ + \frac{1}{2}(k_0 - \Delta k(x_i))\,\Delta t P_{CW}(\hat{x}, x_{i-1}, t_{i-1}) \end{aligned} \tag{S6}$$

$$\begin{aligned} P_{CW}(\hat{x}, x_i, t_i) = [1 - (k_0 - \Delta k(x_i))\,\Delta t] P_{CW}(\hat{x}, x_{i-1}, t_{i-1}) \\ + (k_0 + \Delta k(x_i))\,\Delta t P_{CCW}(-\hat{x}, x_{i+1}, t_{i-1}) \end{aligned} \quad , \tag{S7}$$

$$\begin{aligned} P_{CW}(-\hat{x}, x_i, t_i) = [1 - (k_0 + \Delta k(x_i))\,\Delta t] P_{CW}(-\hat{x}, x_{i+1}, t_{i-1}) \\ + (k_0 - \Delta k(x_i))\,\Delta t P_{CCW}(\hat{x}, x_{i-1}, t_{i-1}). \end{aligned} \tag{S8}$$

This set of equations is again consistent with Eqs. 10-13 in the continuum limit.

In the calculation, we assigned $\Delta x = 0.1$, $2L = 200$ or $2000\Delta x$, $\Delta t = 1$, and $v = \Delta x/\Delta t = 0.1$. Using the computational step Δt as the basic time unit, we defined the transition rates, $k_0 = 0.1$ and $\Delta k = 0.01$, giving the drift velocity $v_d = v\Delta k/k_0 = 10^{-2}$. The equations are solved using the reflective boundary conditions at $x = \pm L$. To generate the numerical solutions in Fig. 1, Eqs. S3-S4 and Eqs. S5-S8 were solved using the initial conditions $P(\pm\hat{x}, x_i, 0) = \exp(-x_i^2/2\sigma^2)/2\sqrt{2\pi\sigma^2}$ and $P_{CCW}(\pm\hat{x}, x_i, 0) = P_{CW}(\pm\hat{x}, x_i, 0) = \exp(-x_i^2/2\sigma^2)/4\sqrt{2\pi\sigma^2}$, respectively. Here, $\sigma = 5\Delta x$ was used. To obtain the numerical solutions in Fig. 2, the initial conditions $P(\pm\hat{x}, x_i, 0) = 1/(4L/\Delta x)$ and $P_{CCW}(\pm\hat{x}, x_i, 0) = P_{CW}(\pm\hat{x}, x_i, 0) = 1/(8L/\Delta x)$ were used for the 2-step and 3-step swimmers, respectively.

Calculations For an Initially Uniform Bacterial Distribution

In most of laboratory experiments the initial bacterial concentration is uniform and the profile evolves under the influence of an imposed chemical gradient. We therefore extend our calculation in the main text to this useful situation. In one dimension, the bacterial profile at $t = 0$ is given by $P(x, 0) = 1/2L$, and the Fourier coefficients are given by,

$$\begin{cases} A_n = & 2q'q_n\psi_{0n}^3 \sinh(q'L)\cos(q_nL), \\ B_m = & 2q'q_m\phi_{0m}^3 \cosh(q'L)\sin(q_mL). \end{cases} \tag{S9}$$

The analytical and numerical results are plotted in Fig. S1, where the designations of colored symbols and lines are identical to that of Fig. 1. We noticed that in this case the bacterial profiles develop near the boundaries first and then spread into the interior of the sample. The problem in hand involves multiple length scales, L, q'^{-1}, and $q_{m,n}^{-1}$, and it is useful to know their corresponding time scales in an experiment. Eq. 20 makes it clear that the relaxation rate for the attainment of a quasi-steady state is given by $\lambda_0 = Dq'^2 = v_d^2/4D$. Since $v_d = v(\Delta k/k_0)$ and $D = v^2/(\epsilon k_0)$, we found $\lambda_0 = \frac{\epsilon k_0}{4}\left(\frac{\Delta k}{k_0}\right)^2$, where $\epsilon = 1$ for *E. coli* and $\epsilon = 2$ for *V. alginolyticus*. This indicates that the profile formation time λ_0^{-1} is essentially independent of the bacterial swimming speed v but depends on the switching rate k_0, the sensitivity characterized by $\Delta k/k_0$, and the motility pattern specified by ϵ. Due to the relatively large system size in a typical experiment or in a natural habitat, $L \gg q'^{-1}$, the drift time L/v_d on the scale of the system size, or for that matter the diffusion time L^2/D, is irrelevant. For a large system, therefore, it is expected that a quasi-steady state with a defined profile develops near the peak of the chemical profile over the time scale λ_0^{-1}. For longer times, $\lambda_0^{-1} < t < L/v_d$, the profile increases in amplitude with its exponential form $\sim \exp(2q'x)$ more-or-less preserved. Our calculation displayed in Fig. S1 is consistent

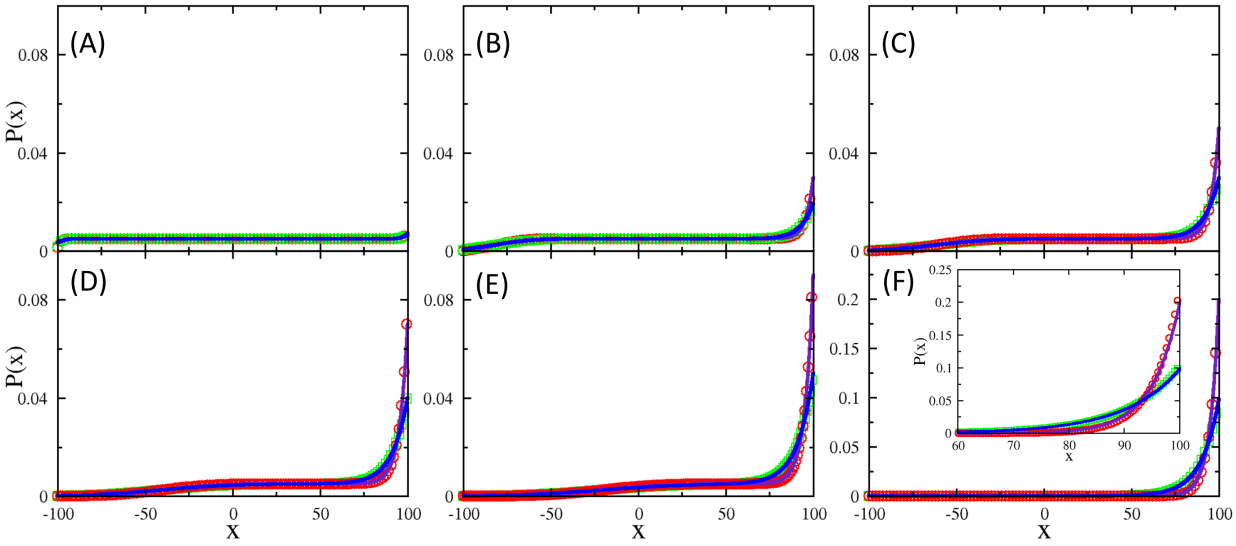

Figure S1: Evolution of $P(x,t)$ starting from the flat distribution $P(x,0) = 1/2L$ in the presence of a linear chemoattractant gradient in the $+\hat{x}$ direction. The bacterial profiles of the 2-step (blue lines) and 3-step (purple lines) swimmers, calculated based on Eq. 18 at reduced times $t/t_v = 0.01$, 0.2, 0.4, 0.6, 0.8, and 2, are plotted in (A-F) respectively. The numerical results based on Eqs. 3-4 and 10-13 are plotted using green squares and red circles for the 2-step and 3-step swimmers. The inset in (F) is the close-up view of the same figure. Note that the shapes of the bacterial profiles near the peak of the chemical concentration $x = L$ form at early t where $t/t_v \ll 1$. Afterward, the peak grows in height but the shapes of the profiles remain more-or-less the same.

with this picture, where $\lambda_0^{-1} = 4000\Delta t$ and $2000\Delta t$ for the 2-step and 3-step swimmer, respectively.

The Memory Effect

Bacteria detect chemical gradients by temporal comparison. Processing of the chemical signals typically introduces a time delay in response. Such a delay in general reduces the drift velocity of the cell. This is because if a cell's swimming direction is reversed at a certain moment, immediately after the reversal, the gradient "computed" by the cell is opposite to the gradient currently experienced by the cell due to the delay (1). For example, if the cell swims up an attractant gradient before it goes down the gradient due to a direction

randomization, within the memory time right after the reversal, dc/dt computed by the cell is still positive. As a result, instead of increasing the switching rate, the cell reduces the switching rate and its average displacement down the gradient is extended. Similarly, right after a cell switches from going down to going up the gradient, its average displacement up the gradient is decreased. The memory effect can be taken into consideration systematically as demonstrated by de Gennes (2). Based on the molecular and functional aspects of *E. coli* chemotaxis (3, 4) and using a linear response, the change in the switching rate Δk depends on the history of chemical exposure and can be mathematically expressed as,

$$\frac{\Delta k(t)}{k_0} = \int_{-\infty}^{t} R(t-t')c(t')dt'. \tag{S10}$$

In the above, $c(t)$ is the chemical concentration sensed by the bacterium at time t, and $R(t)$ is the response function given by

$$R(t) = R_0 \frac{\tau_Z \tau_m}{\tau_m - \tau_Z}\left(\frac{1}{\tau_Z}\exp(-t/\tau_Z) - \frac{1}{\tau_m}\exp(-t/\tau_m)\right), \tag{S11}$$

where τ_Z and τ_m are respectively the dephosphorylation and methylation times, and R_0 is the amplitude of the response.

For the 2- and 3-step swimmers having the same swimming speed v and the same response $R(t)$, it can be shown using the results in Refs. (1, 2) that the ratio of the drifting velocities for the two bacteria is given by,

$$\frac{v_V}{v_E} = \frac{1}{2}\left(\frac{1}{1+k_0\tau_Z} + \frac{1}{1+k_0\tau_m}\right). \tag{S12}$$

The effect of memory on bacterial chemotaxis and in particular on the drift velocity have also been considered by Taktikos et. al (5). It was assumed that the chemotactic response function has a typical time scale k_0^{-1} (see Eq. 26 of Ref. (5)). With such an assumption, Eq. S12 yields $v_V \approx \frac{1}{2}v_E$ for $k_0\tau_Z \approx 1$ and $k_0\tau_m \approx 1$, which is consistent with Eq. 28 of Ref. (5). Thus, bacterial memory generally makes 3-step swimmers drift slower in a linear chemical

gradient than their 2-step counterparts unless the bacteria can process the chemical signal rapidly with $k_0\tau_Z \ll 1$ and $k_0\tau_m \ll 1$. In this case the drifting velocity of a 3-step swimmer would not be compromised by the delay, and one obtains the result $v_V \approx v_E$.

Supporting References

1. Altindal, T., L. Xie, and X.-L. Wu, 2011. Implications of Three-Step Swimming Patterns in Bacterial Chemotaxis. *Biophys. J.* 100:32–41.

2. de Gennes, P., 2004. Chemotaxis: the role of internal delays. *Eur. Biophys. J.* 33:691–693.

3. Tu, Y., T. Shimizu, and H. Berg, 2008. Modeling the chemotactic response of *Escherichia coli* to time-varying stimuli. *Proc. Natl. Acad. Sci. USA* 105:14855.

4. Celani, A., T. Shimizu, and M. Vergassola, 2011. Molecular and Functional Aspects of Bacterial Chemotaxis. *J. Stat. Phys.* 144:219–240.

5. Taktikos, J., H. Stark, and V. Zaburdaev, 2013. How the Motility Pattern of Bacteria Affects Their Dispersal and Chemotaxis. *PLoS ONE* 8:e81936.